



Gas Sensor Investigations through Adsorption of Toxic Gas Molecules on Single and Double Vacancy Graphene

Salah Abdul Mahdi Khudair^{1*}, Ameen Alwan Mohaimeed²

Abstract

The interactions existing between 2 distinctive small molecules of the gas (CO, NO₂ and NH₃) and graphene (double and single vacancy graphene) were examined with utilizing the Density Functional Theory (DFT) computations for the purpose of exploring their possible gas sensor applications. Also, electronic and structural characteristics of the adsorption adducts of the graphene molecules were on a basis of molecular adsorption configurations and graphene structures, while the resulted electronic structure regarding each of the adsorbed systems was markedly different. In addition, the results are showing that adsorption of (NO₂, NH₃ and CO) on single vacancy graphene (SVG) and (CO and NH₃) on double vacancy graphene (DVG) are weak physisorption with an adsorption energy (E_{ad}) ranging from (-0.207 to -0.922) eV. The article demonstrates the feasibility of SVG might be excellent sensor for (NO₂, NH₃ and CO) and DVG might be excellent sensor for (NH₃ and CO). At the same time, the adsorption related to (NO₂) on the DVG was strong chemisorption. Furthermore, this gas's strong interactions on DVG is showing that the DVG might be activate or catalyse, proposing the probability of DVG as one of the metal free catalysts, such work indicates that sensitivity regarding graphene-based chemical sensors of gas might be considerably enhanced via the introduction of the suitable defects.

87

Key Words: Electronic Properties, DFT, Adsorption, Vacancy Graphene, Gas Sensor, Density of States.

DOI Number: 10.14704/nq.2020.18.9.NQ20221

NeuroQuantology 2020; 18(9):87-95

Introduction

Air pollution can be defined as one of the serious problems related to the health of humans, also detecting the toxic gases is of high importance in ecological balance, monitoring the environment and industrial productions.¹⁻³ The more and more increase in the emissions of toxic as well as greenhouse gases such as NO₂, NH₃ and CO because of many domestic and industrial activities resulted in major threats to environment and human health,⁴ thus, many studies were focusing on developing adequate solid state gas sensors. Good solid-state gas sensor must be having

excellent sensitivity, low cost of production as well as miniature sizes.⁵⁻⁷ Typically, excellent gas sensors must have high sensitivity and selectivity, due to the fact that high selectivity has the ability of providing rapid responses to specific target gas, while the high sensitivity has the ability of improving the limit of detection.^{8,9} In addition, the graphene was specified as a promising material for a lot of practical applications¹⁰⁻¹⁶.

Corresponding author: Salah Abdul Mahdi Khudair

Address: ^{1,2}Directorate of Education Babylon, Ministry of Education, Iraq.

^{1*}E-mail: salahalmahdi30@gmail.com

Relevant conflicts of interest/financial disclosures: The authors declare that the research was conducted in the absence of any commercial or financial relationships that could be construed as a potential conflict of interest.

Received: 27 July 2020 **Accepted:** 24 August 2020



With regard to applications of gas sensing, the pristine graphene showed low adsorption energy values to detect many gas molecules due to its inactive surface.¹⁷⁻²⁰ On the contrary, the existence of defects in the graphene lead to chemisorption regarding gas molecules²¹⁻²³. For example, a study conducted by Sanyal et al. Have theoretically examined the dissociations related to N₂ molecule at divacancy in the graphene²⁴. Comparable adsorptions related to the molecule's dissociations at monovacancy in the graphene have been indicated for H₂,²⁵ O₂,²⁶ and H₂S.^{27,28} Past studies are suggesting that the gases adsorption might be improved via changing the graphene structures through creating vacancies.^{21,29} In certain experimental study, a study conducted by Zhang et al showed improved sensing efficiency following providing single carbon vacancy defects in graphene.²¹ For the total exploitation of the potential of graphene sensors, there is high importance in understanding the interactions between adsorbed molecules and graphene surface. Theoretical researches were carried out for examining the adsorptions related to small molecules on the graphene. The majority of past works were focusing on perfect graphene, also anticipated fairly low adsorption energies compared to essential requirements of the gas sensing applications.³⁰⁻³² In the presented study, there are 2 distinctive graphene-based sensing materials are established. Furthermore, adsorptions of the molecules of (NO₂, NH₃ and CO) on DVG and SVG were examined. Also, the electronic properties and adsorption energy have been evaluated for examining the interactions between the two graphene sheets and gas molecules.

Computational Approaches

The calculations have been conducted in this work utilizing DFT in Generalized Gradient Approximation (GGA).^{33,34} Also, the geometric structures have been totally optimized utilizing Gaussian 09 program package. We chose the Perdew, Burke, and Ernzerhof (PBE) exchange correlation functional³³ for a purpose of describing the correlation energy and exchange in total energy calculations and structural optimizations. For examining the adsorption mechanisms regarding gas molecules on DVG and SVG, the system has

been modeled as (3×3) supercell of graphene, SVG (41 C atoms) through eliminating single carbon atom at graphene surface center, also DVG (40 C atoms) through eliminating 2 neighboring atoms of carbon at graphene's center. As the surface of the graphene was extremely inactive, the formation regarding DV and SV in graphene lead to dangling bonds at vacancy.³⁵ Actually, the molecule's binding energy on the surface is revealing the adsorption type (chemisorption or physisorption) occurs between surface and molecule. Also, the physisorption was considered as one of the reversible processes, while the chemisorption could be irreversible particularly in the case when being related to the molecule's dissociation.^{36,37} For evaluating the interactions between adsorption sheet surface and gas molecules, E_{ad} for adsorbed systems was calculated, that is defined as Eq:³⁸

$$E_{ad} = E_{\text{graphene} + \text{gas molecule}} - (E_{\text{graphene}} + E_{\text{gas molecule}}) \quad (1)$$

In which the E_{graphene + GasMolecule} has been defined as the total energy related to relaxed molecule on graphene, also the E_{graphene} has been the energy regarding isolated graphene, and E_{gasmolecule} represents energy which is related to isolated gas molecule. In addition, the diversity of relative energy of lowest unoccupied molecular orbital (LUMO) and highest occupied molecular orbital (HOMO) of free DVG & SVG and adsorbed molecule on DVG and SVG provides the interaction mechanism. HOMO might be specified as electron donor due to having excess amount of the electrons, while LUMO lacks electrons and thus it has the power of accepting electrons.

Results and Discussions

1) Electronic Structure of SVG and DVG

The native defects in 2-D layered materials is of high importance to tune their electronic and structural characteristics to large extent.^{8,39-41} In the presented section, DFT simulations have been performed for characterizing the electronic characteristics of DVG and SVG, and the improved models were indicated in Figure. 1 (a) and (b), while the carbon atoms in graphene sheet were eliminated, are efficient ways for modifying the electronic and structural characteristics of graphene. SVG and DVG retain the planar form after full relaxation and their corresponding model have been illustrated in Fig. 1 a&b.



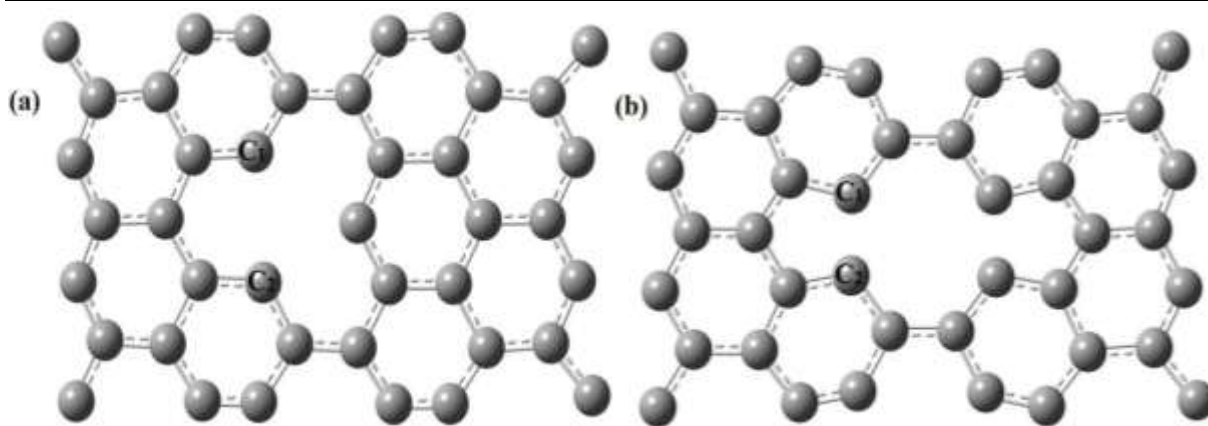


Fig. 1. Model of SVG (a) and DVG (b)

Table I clarifies the impacts of defects with SVG and DVG on graphene’s electronic properties. SVG has large values of E_g , E_{HOMO} , E_{LUMO} and E_F compared with DVG. As is clear from the table, E_F that is estimated from E_{HOMO} and E_{LUMO} ($E_F = (E_{HOMO} + E_{LUMO})/2$) equal to -5.370eV and -5.344eV for SVG and DVG, respectively.

Table I. Electronic characteristics of SVG and DVG

Property (eV)	SVG	DVG
E_g	0.043	0.006
E_{HOMO}	-5.391	-5.348
E_{LUMO}	-5.348	-5.341
E_F	-5.370	-5.344

There have been many main peaks in valence as well as conduction band, Fig. 2 (a) and (b) are showing the density of states (DOS), the maximum amount of the degenerate states in valence and conduction bands was 3 for DVG and 4 for SVG. Also, it was indicated that there were states provided for the occupation at elevated levels of the DOS for certain level of energy, while there aren’t any states which might be occupied at zero- DOS for the level of the energy. In addition, defects with the SVG result in insignificant increase in DOS in valence and conduction bands compared to those of DVG, as seen in Fig. 2.

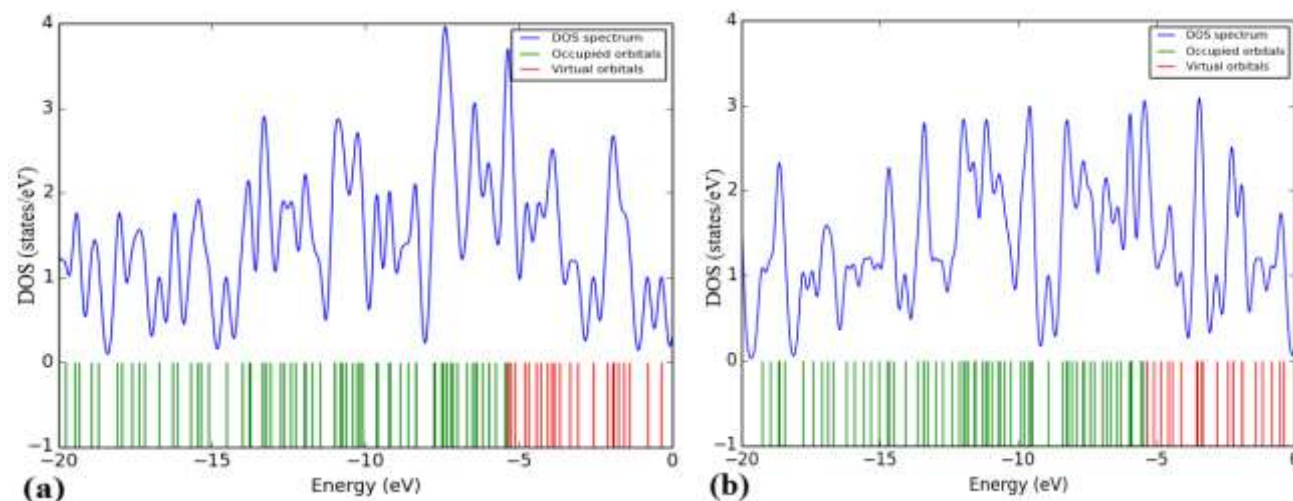


Fig. 2. Density of states for: (a) SVG and (b) DVG. Alpha DOS spectrum in red line, and beta DOS spectrum in blue line

2) Gas Molecules Adsorption on SVG and DVG

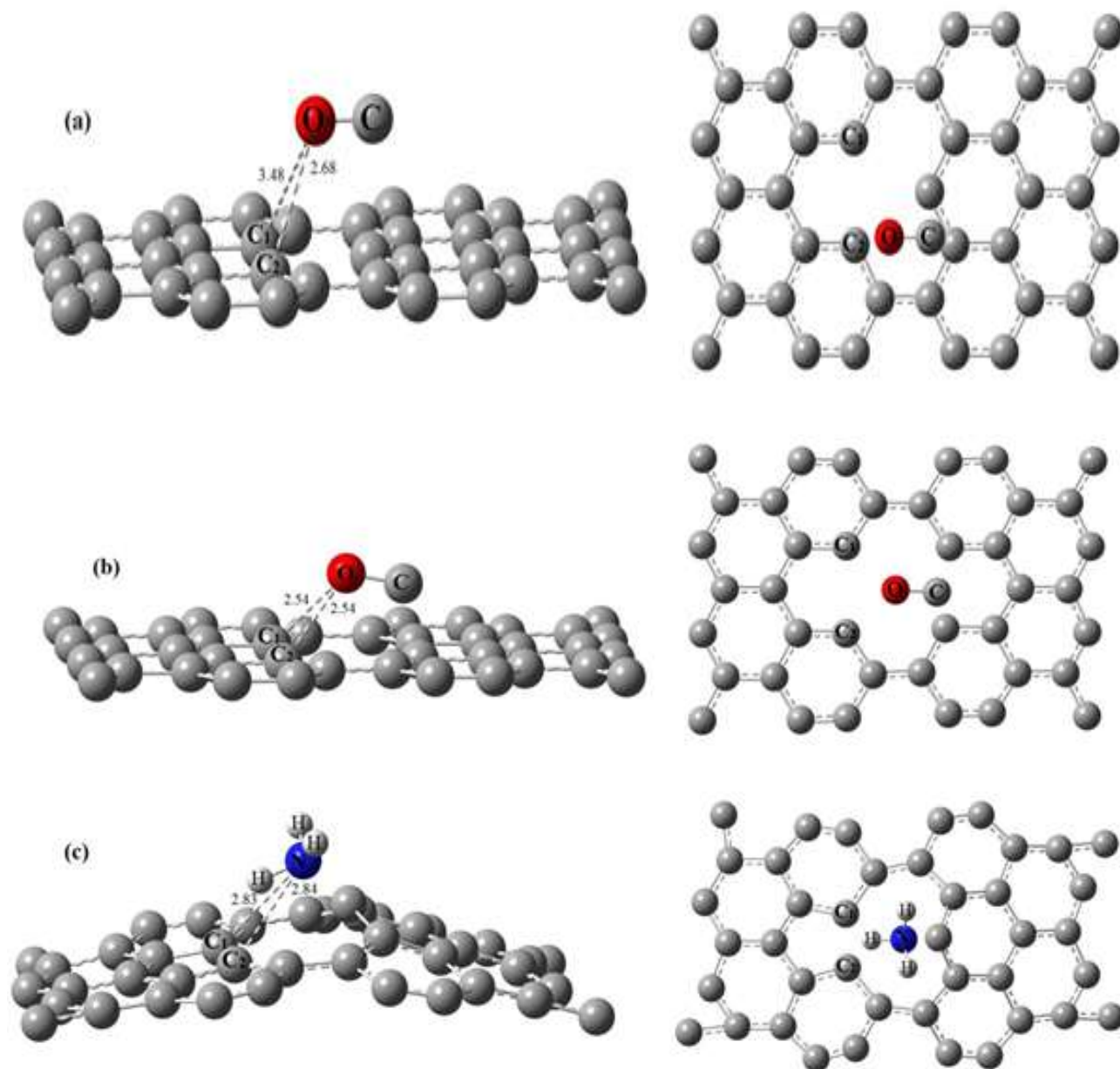
For the purpose of finding the major important configurations of the adsorption, the examined molecule has been originally placed at various positions over graphene sheet with a variety of the orientation values. Following full relaxation, the

enhanced configurations which have been acquired from various initial states have been put to comparison for identifying the major energetically stable one. In addition, the major stable configurations related to NO_2 , NH_3 and CO molecules on DVG and SVG were showed in Figure. 3. Thorough information from the simulation



related to various molecules on the graphene systems, involving the adsorption energy values, were provided in table II. Following the adsorption of such gases, its impact will be examined on structural and electronic characteristics of the DVG and SVG. Also, the optimized adsorption structures which are related to CO adsorbed on DVG and SVG are showed in Figures. 3(a) and (b). At the same time, the bond lengths will be examined for CO

which is adsorbed on the SVG of C₁-O and C₂-O were 3.48Å and 2.68Å, respectively, therefore the values were consistent with the other results for bond length of C₁-O,⁴² whereas the bond lengths with regard to CO adsorbed on the DVG of C₁-O as well as C₂-O were 2.54Å and 2.54Å, respectively. Meanwhile the angles of C₁-O- C₂ of CO adsorbed on SVG and DVG are 45° and 59°, respectively.



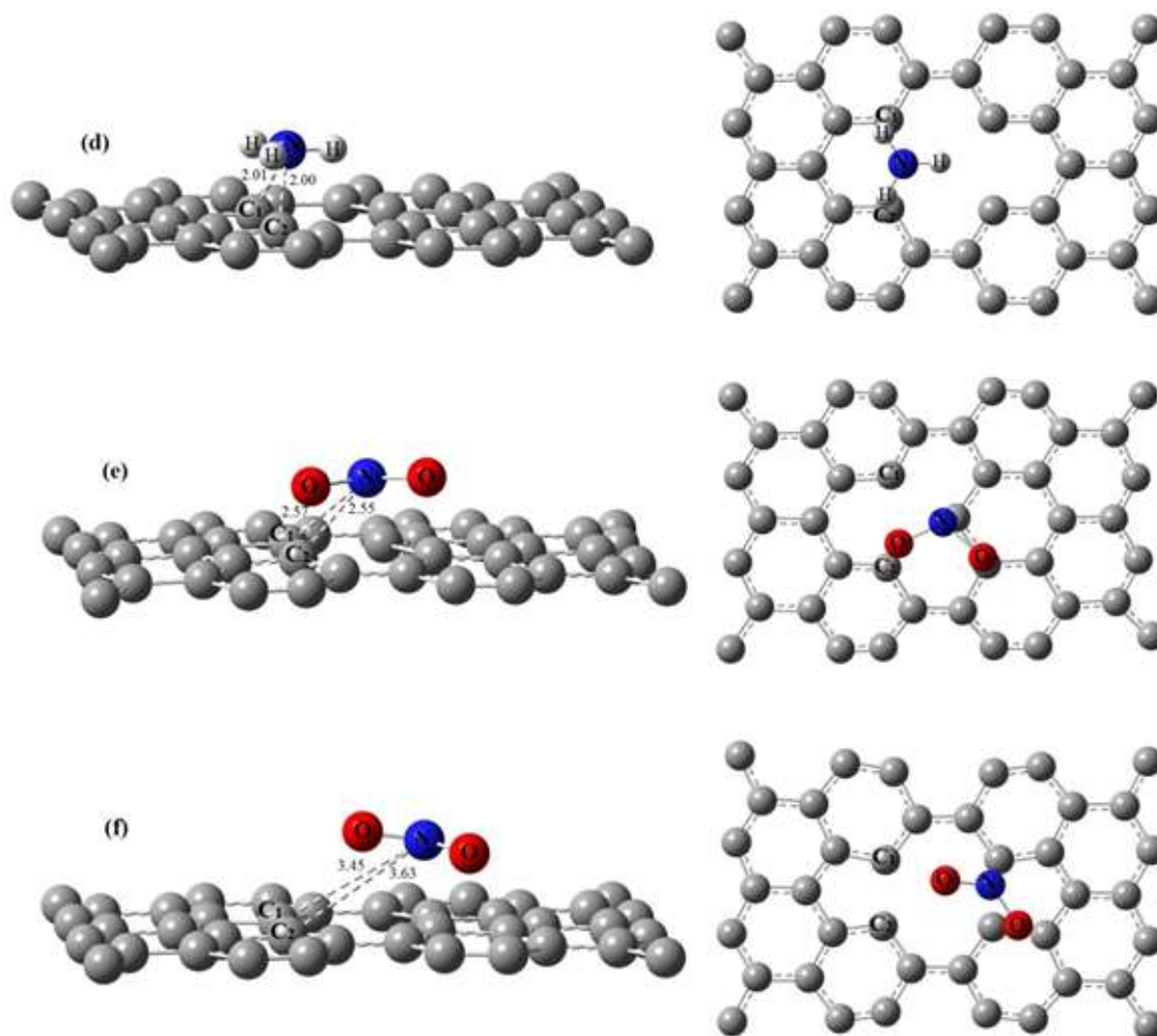


Fig. 3. Top and side view of the optimized structures and key bond length of gas molecules (a) CO, (c) NH₃ and (e) NO₂ adsorbed on SVG, (b) CO, (d) NH₃ and (f) NO₂ adsorbed on DVG.

It can be noticed from Table II, the E_g for adsorption of CO on SVG and DVG is larger than those of SVG and DVG, this point out that the E_g increases with the adsorption of CO on SVG and DVG. The computed E_F for adsorption of CO on SVG and DVG is larger than the calculated value for SVG and DVG. It has been found that the E_{HOMO} for adsorption of CO on SVG and DVG is larger than those of SVG and DVG, and E_{LUMO} for adsorbed SVG is larger than those of SVG, while E_{LUMO} for adsorbed DVG was smaller compared to those of DVG. The results are showing that high value related to E_{HOMO} was -5.478eV, such values is indicating the molecule's tendency to donate electrons. E_{ad} for adsorption of CO on SVG and DVG are 0.548eV and 0.422eV corresponding to weak physisorption.⁴³ The binding strength of CO with SVG and DVG are intermediate with the values of E_{ad} . Thus, SVG and

DVG might be effectively utilized for detecting CO as the adsorption desorption equilibrium regarding CO on DVG and SVG were built easily.

Table II. Electronic and Structural properties of different gases adsorbed on SVG and DVG

Device	Gas	E_{ad} (eV)	E_g (eV)	E_{HOMO} (eV)	E_{LUMO} (eV)	E_F (eV)
SVG	CO	0.548	0.083	-5.436	-5.353	-5.395
	NH ₃	-0.398	0.022	-5.056	-5.034	-5.045
	NO ₂	-0.207	0.290	-5.431	-5.141	-5.286
DVG	CO	0.422	0.171	-5.478	-5.306	-5.392
	NH ₃	-0.922	0.101	-5.496	-5.394	-5.445
	NO ₂	-1.124	0.036	-5.591	-5.555	-5.573

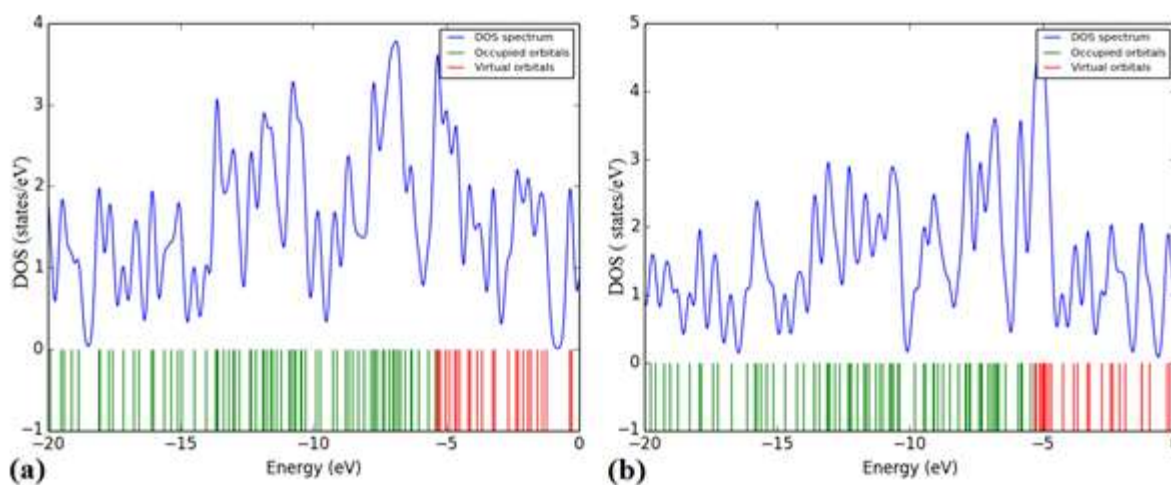


The NH_3 molecule is adsorbed to SVG and DVG, as seen in Figures 3(c) & (d), from this figure, we notice that the adsorption of NH_3 on SVG leads to a distortion in planar structure of the graphene sheet, in return, DVG retain the planar form after the adsorption of NH_3 . The bond lengths for NH_3 adsorbed on SVG of $\text{C}_1\text{-N}$ and $\text{C}_2\text{-N}$ are 2.83\AA and 2.84\AA , respectively, such values were in accordance with other results for the bond lengths of $\text{C}_1\text{-N}$ and $\text{C}_2\text{-N}$,²¹ while that bond lengths for NH_3 adsorbed on DVG of $\text{C}_1\text{-N}$ and $\text{C}_2\text{-N}$ are 2.01\AA and 2.00\AA , respectively, meanwhile the angles of $\text{C}_1\text{-N-C}_2$ of NH_3 adsorbed on SVG and DVG are 33° and 75° , respectively. The overall results of adsorbed NH_3 on SVG and DVG are summarized in Table II. The adsorption energies indicate that binding strength regarding NH_3 with DVG and SVG is intermediate with E_{ad} (-0.922 and -0.398eV). Thus, SVG and DVG can be used to detect NH_3 . It is obvious from Tables I and II the adsorbed DVG leads to increase the E_g in comparison with DVG, while that adsorbed SVG leads to decrease the E_g in comparison with SVG. The table shows the calculated E_{HOMO} and E_{LUMO} of adsorption of NH_3 on SVG are smaller than those of SVG, in return, E_{HOMO} and E_{LUMO} of adsorption of NH_3 on DVG are larger than those of DVG. The computed E_F for adsorption of NH_3 on SVG is smaller than the calculated value for SVG, while that E_F for adsorption of NH_3 on DVG is larger than the calculated value for DVG.

The NO_2 molecules are adsorbed to SVG and DVG, as can be seen in the Figure. 3(e) and (f). The optimised bond lengths for NO_2 adsorbed on SVG of $\text{C}_1\text{-N}$ and $\text{C}_2\text{-N}$ are 2.57\AA and 2.55\AA , respectively, while that bond lengths for NO_2 adsorbed on DVG of $\text{C}_1\text{-N}$ and $\text{C}_2\text{-N}$ are 3.45\AA and 3.63\AA , respectively, at the same time that angles of $\text{C}_1\text{-N-C}_2$ of NO_2 adsorbed on SVG and DVG are 62° and 30° ,

respectively. Table II lists the results of adsorption of NO_2 on SVG and DVG, it can be noticed that the E_g increases with the adsorption of NO_2 on SVG and DVG in comparison with of SVG and DVG. We found the adsorption related to NO_2 on the SVG was weak physisorption, with E_{ad} being equal to -0.207eV , also the binding strength related to NO_2 with the SVG was intermediate with value of E_{ad} . Therefore, the SVG might be effectively utilized for detecting NO_2 as adsorption desorption equilibrium regarding NO_2 on SVG was built easily. Conversely, DVG was strong chemisorption with E_{ad} more than 1eV , therefore, the DVG is not suitable as a sensor of NO_2 , rather than DVG might be activating such adsorbate, indicating the probability of DVG as catalyst. The calculated E_{HOMO} of adsorption of NO_2 on SVG is larger than SVG, while E_{LUMO} of adsorption of NO_2 on SVG is smaller than SVG, conversely, E_{HOMO} and E_{LUMO} of adsorption of NO_2 on DVG are larger than DVG. E_F for adsorption of NO_2 on SVG is smaller than the calculated value for SVG, while E_F for adsorption of NO_2 on DVG is larger than DVG.

For the purpose of identifying the impact of defects on the E_{ad} , DOS of DVG and SVG with adsorbed CO were estimated in Fig4(a) & (b), the Figure is showing that DOS of DVG and SVG with adsorption related to gas molecules CO were distinctive from DVG and SVG, the reference to SVG, the maximum peaks become less, for instance, the valence and conduction bands were considered less with maximum number of DOS, on the other hand, DOS to the adsorbed DVG, the highest of peaks will be higher, for instance, the valence and conduction bands were higher with highest number of DOS. At the same time, the showing DOS to the adsorption NH_3 on SVG and DVG result in increasing the DOS in the bands of valence and conduction compared to DOS of DVG and SVG, as shown in Fig4(c) & (d).



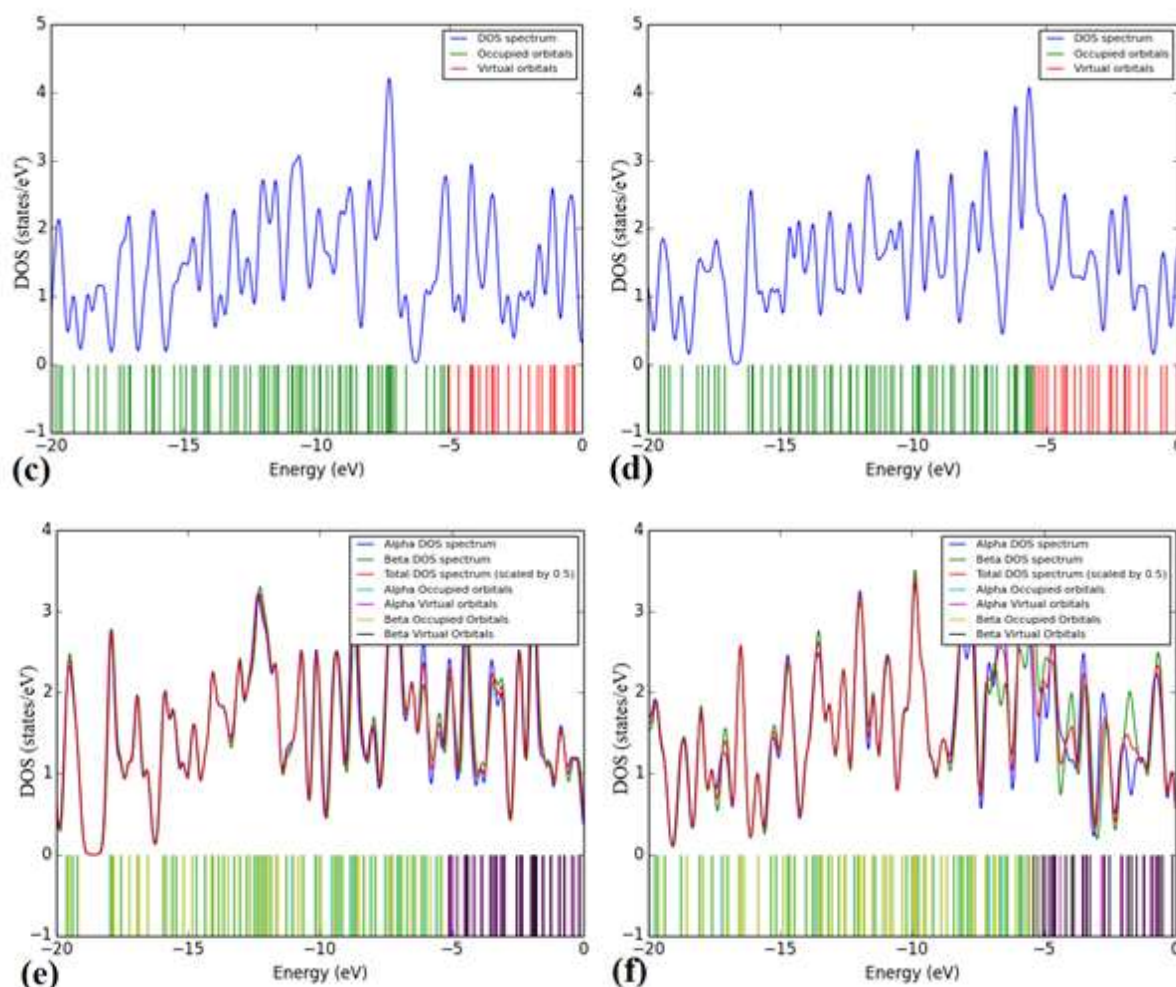


Fig. 4. DOS for adsorbate (a) CO, (c) NH₃ and (e) NO₂ on SVG, (b) CO, (d) NH₃, and (f) NO₂ on DVG.

Finally, DOS for adsorption of NO₂ on SVG result in decreasing the DOS in the bands of valence and conduction compared to DOS of SVG, none-the-less, DOS for adsorption of NO₂ on DVG result in increasing the DOS in valence and conduction compared to DOS of DVG, as seen in Fig4(e) and (f).

Conclusions

In brief, adsorption which is related to NO₂, NH₃, and CO DVG and SVG was examined. We implemented first principles computations for clarifying the effects of defects on graphene as one of the gas sensor materials. It has been indicated that the existence of vacancy defects has the ability of enhancing E_{ad} of NO₂, NH₃ and CO molecules in a region that is near the defect due to the introduction of extra potential trap. In addition, it might be indicated that adsorption of NO₂, NH₃ & CO gas molecules on SVG are undergoing weak physisorption interactions with moderate E_{ad} . Consequently, SVG could be good sensor for NO₂,

NH₃ and CO. Also, the adsorption related to gas molecule NO₂ on DVG is undergoing strong chemisorption interactions, so it presumably unsuitable for usage as gas sensor for NO₂, the DVG might be activate or catalyse, which suggest the potential of DVG as catalyst, while the adsorption related to NH₃ and CO on DVG were weak physisorption interactions with moderate E_{ad} , therefore it can be used as a good sensor for these gases. Thus, there are 3 molecules showing physisorption on DVG and SVG with low-adsorption energies, which is suggesting that the unmodified graphene wasn't perfect material for gas sensing. The presented is showing that sensitivity and selectivity of graphene based gas sensor types might be considerably improved via providing defects into graphene, that might be utilized for designing chemical sensors, and graphene might be utilized for building sensors to detect particular molecules.

References

- Pearce R, Yakimov T, Andersson M, Hultman L, Spetz AL, Yakimova R. Epitaxially grown graphene based gas sensors for ultra sensitive NO₂ detection. *Sensors and Actuators B: Chemical* 2011; 155(2): 451-455.
- Qin Y, Sun X, Li X, Hu M. Room temperature NO₂-sensing properties of Ti-added nonstoichiometric tungsten oxide nanowires. *Sensors and Actuators B: Chemical* 2012; 162(1): 244-250.
- Hosseini-Babaei F, Amini A. A breakthrough in gas diagnosis with a temperature-modulated generic metal oxide gas sensor. *Sensors and Actuators B: Chemical* 2012; 166: 419-425.
- Esrafil MD. Boron and nitrogen co-doped graphene nanosheets for NO and NO₂ gas sensing. *Physics Letters A* 2019; 383(14): 1607-1614.
- Capone S, Forleo A, Francioso L, Rella R, Siciliano P, Spadavecchia J, Presicce DS, Taurino AM. Solid State Gas Sensors: State of the Art and Future Activities. *Journal of Optoelectronics and Advanced Materials* 2003; 5(5): 1335-1348.
- Barsan N, Koziej D, Weimar U. Metal oxide-based gas sensor research: How to?. *Sensors and Actuators B: Chemical* 2007; 121(1): 18-35.
- Kolmakov A, Moskovits M. Chemical sensing and catalysis by one-dimensional metal-oxide nanostructures. *Annual Review of Materials Research* 2004; 34: 151-180.
- Varghese SS, Lonkar S, Singh KK, Swaminathan S, Abdala A. Recent advances in graphene based gas sensors. *Sensors and Actuators B: Chemical* 2015; 218: 160-183.
- Wei W, Li W, Wang L. High-selective sensitive NH₃ gas sensor: A density functional theory study. *Sensors and Actuators B: Chemical* 2018; 263: 502-507.
- Avouris P. Graphene: electronic and photonic properties and devices. *Nano letters* 2010; 10(11): 4285-4294.
- Gilje S, Han S, Wang M, Wang KL, Kaner RB. A Chemical Route to Graphene for Device Applications. *Nano Letters* 2007; 7(11): 3394-3398.
- Novoselov KS, Geim AK, Morozov SV, Jiang D, Katsnelson MI, Grigorieva IV, Dubonos SV, Firsov AA. Two-dimensional gas of massless Dirac fermions in graphene. *Nature* 2005; 438(7065): 197-200.
- Bae S, Kim H, Lee Y, Xu X, Park J, Zheng Y, Balakrishnan J, Lei T, Kim HR, Song YI, Kim Y, Kim KS, Özyilmaz B, Ahn J, Hong BH, Iijima S. Roll-to-roll production of 30-inch graphene films for transparent electrodes. *Nature Nanotechnology* 2010; 5(8): 574-578.
- Petrone N, Dean CR, Meric I, Van Der Zande AM, Huang PY, Wang L, Hone J. Chemical vapor deposition-derived graphene with electrical performance of exfoliated graphene. *Nano letters* 2012; 12(6): 2751-2756.
- Yuan W, Shi G. Graphene-based gas sensors. *Journal of Materials Chemistry A* 2013; 1(35): 10078-10091.
- Ko G, Kim HY, Ahn J, Park YM, Lee KY, Kim J. Graphene-based nitrogen dioxide gas sensors. *Current Applied Physics* 2010; 10(4): 1002-1004.
- You Y, Deng J, Tan X, Gorjizadeh N, Yoshimura M, Smith SC, Joshi RK. On the mechanism of gas adsorption for pristine, defective and functionalized graphene. *Physical Chemistry Chemical Physics* 2017; 19(8): 6051-6056.
- Caffrey NM, Armiento R, Yakimova R, Abrikosov IA. Changes in work function due to NO₂ adsorption on monolayer and bilayer epitaxial graphene on SiC (0001). *Physical Review B* 2016; 94(20): 205411.
- Zou Y, Li F, Zhu ZH, Zhao MW, Xu XG, Su XY. An ab initio study on gas sensing properties of graphene and Si-doped graphene. *The European Physical Journal B* 2011; 81(4): 475-479.
- Jappor HR, Khudair SAM. Electronic properties of adsorption of CO, CO₂, NH₃, NO, NO₂ and SO₂ on nitrogen doped graphene for gas sensor applications. *Sensor Letters* 2017; 15(5): 432-439.
- Zhang YH, Chen YB, Zhou KG, Liu CH, Zeng J, Zhang HL, Peng Y. Improving gas sensing properties of graphene by introducing dopants and defects: a first-principles study. *Nanotechnology* 2009; 20(18): 185504.
- Jappor HR, Khudair SAM. Al-doped graphene as a sensor for harmful gases (CO, CO₂, NH₃, NO, NO₂ and SO₂). *Sensor Letters* 2017; 15(12): 1023-1030.
- Khudair SAM, Jappor HR. Adsorption of Gas Molecules on Graphene Doped with Mono and Dual Boron as Highly Sensitive Sensors and Catalysts. *Journal of Nanostructures* 2020; 10(2): 217-229.
- Sanyal B, Eriksson O, Jansson U, Grennberg H. Molecular adsorption in graphene with divacancy defects. *Physical Review B* 2009; 79(11): 113409.
- Ricco M, Pontiroli D, Mazzani M, Choucair M, Stride JA, Zazyev OV. Muons probe strong hydrogen interactions with defective graphene. *Nano letters* 2011; 11(11): 4919-4922.
- Kaloni TP, Cheng YC, Faccio R, Schwingenschlögl U. Oxidation of monovacancies in graphene by oxygen molecules. *Journal of Materials Chemistry* 2011; 21(45): 18284-18288.
- Hegde VI, Shirodkar SN, Tit N, Waghmare UV, Yamani ZH. First principles analysis of graphene and its ability to maintain long-ranged interaction with H₂S. *Surface science* 2014; 621: 168-174.
- Kouser S, Waghmare UV, Tit N. Adsorption and splitting of H₂S on 2D-ZnO 1- x N y: first-principles analysis. *Physical Chemistry Chemical Physics* 2014; 16(22): 10719-10726.
- Lee G, Yang G, Cho A, Han JW, Kim J. Defect-engineered graphene chemical sensors with ultrahigh sensitivity. *Physical Chemistry Chemical Physics* 2016; 18(21): 14198-14204.
- Bai L, Zhou Z. Computational study of B-or N-doped single-walled carbon nanotubes as NH₃ and NO₂ sensors. *Carbon* 2007; 45(10): 2105-2110.
- Zhang Y, Zhang Y, Zhang D, Liu C. Novel chemical sensor for cyanides: boron-doped carbon nanotubes. *The Journal of Physical Chemistry B* 2006; 110(10): 4671-4674.
- Bauschlicher Jr CW, Ricca A. Binding of NH₃ to graphite and to a (9,0) carbon nanotube. *Physical Review B* 2004; 70(11): 115409.
- Perdew JP, Burke K, Ernzerhof M. Generalized gradient approximation made simple. *Physical review letters* 1996; 77(18): 3865.
- Peyghan AA, Noei M, Yourdkhani S. Al-doped graphene-like BN nanosheet as a sensor for para-nitrophenol: DFT study. *Superlattices and Microstructures* 2013; 59: 115-122.



- Hashimoto A, Suenaga K, Gloter A, Urita K, Iijima S. Direct evidence for atomic defects in graphene layers. *Nature* 2004; 430(7002): 870-873.
- Cui H, Zhang X, Zhang G, Tang J. Pd-doped MoS₂ monolayer: a promising candidate for DGA in transformer oil based on DFT method. *Applied Surface Science* 2019; 470: 1035-1042.
- Cui H, Zhang X, Chen D, Tang J. Pt & Pd decorated CNT as a workable media for SOF₂ sensing: A DFT study. *Applied Surface Science* 2019; 471: 335-341.
- Akdim B, Duan X, Pachter R. The effects of O₂ adsorbates on field emission properties of single-wall carbon nanotubes: a density functional theory study. *Nano letters* 2003; 3(9): 1209-1214.
- Rajasekaran G, Parashar A. Effect of topological defects on mechanical properties of graphene sheets: a molecular dynamics study. *Materials Today: Proceedings* 2018; 5(2): 6780-6788.
- Vicarelli L, Heerema SJ, Dekker C, Zandbergen HW. Controlling defects in graphene for optimizing the electrical properties of graphene nanodevices. *ACS nano* 2015; 9(4): 3428-3435.
- Shakourian-Fard M, Kamath, G. The effect of defect types on the electronic and optical properties of graphene nanoflakes physisorbed by ionic liquids. *Physical Chemistry Chemical Physics* 2017; 19(6): 4383-4395.
- Yang S, Lei G, Xu H, Xu B, Li H, Lan Z, Gu H. A DFT study of CO adsorption on the pristine, defective, In-doped and Sb-doped graphene and the effect of applied electric field. *Applied Surface Science* 2019; 480: 205-211.
- Feng JW, Liu YJ, Wang HX, Zhao JX, Cai QH, Wang XZ. Gas adsorption on silicene: a theoretical study. *Computational Materials Science* 2014; 87: 218-226.
- Hamid N. The effectiveness of music therapy on depression and happiness of depressed women. *NeuroQuantology* 2019; 17(12): 19-26.
<http://doi.org/10.14704/nq.2019.17.12.NQ19110>
- Alhashimi MTM, Muhsin NMB. Treatment of (Electric wires and machines)-erosion via engineering materials by the coating. *NeuroQuantology* 2019; 17(11): 11-16.
<http://doi.org/10.14704/nq.2019.17.11.NQ19108>

